
Ad-Rec: Advanced Feature Interactions to Address Covariate-Shifts in Recommendation Networks

Muhammad Adnan* Yassaman Ebrahimzadeh Maboud* Divya Mahajan[†] Prashant J. Nair*

{adnan,yassaman,prashantnair}@ece.ubc.ca

divya.mahajan@microsoft.com

The University of British Columbia*

Microsoft[†]

Abstract

Recommendation models are vital in delivering personalized user experiences by leveraging the correlation between multiple input features. However, deep learning-based recommendation models often face challenges due to evolving user behaviour and item features, leading to covariate shifts. Effective cross-feature learning is crucial to handle data distribution drift and adapting to changing user behaviour. Traditional feature interaction techniques have limitations in achieving optimal performance in this context.

This work introduces Ad-Rec, an advanced network that leverages feature interaction techniques to address covariate shifts. This helps eliminate irrelevant interactions in recommendation tasks. Ad-Rec leverages masked transformers to enable the learning of higher-order cross-features while mitigating the impact of data distribution drift. Our approach improves model quality, accelerates convergence, and reduces training time, as measured by the Area Under Curve (AUC) metric. We demonstrate the scalability of Ad-Rec and its ability to achieve superior model quality through comprehensive ablation studies.

1 Introduction

Recommendation models are essential for delivering personalized recommendations in various web services [Koren et al., 2009]. Over time, these models have evolved from conventional collaborative filtering designs [Koren et al., 2009] to deep learning-based approaches [He et al., 2017, Naumov et al., 2019, Zhao et al., 2019, Ishkhanov et al., 2020], leveraging their capacity to capture complex patterns and improve recommendation quality. However, deep learning-based recommendation models face challenges due to covariate shifts caused by dynamic user behaviour and evolving item features [Naumov et al., 2019, Ishkhanov et al., 2020, Guo et al., 2017]. These shifts lead to a misalignment between the training and testing data distributions, resulting in degraded performance and limited generalization. This paper aims to address these challenges.

Deep learning-based recommendation models, shown in Figure 1a, comprise neural networks, embedding lookup, and, most importantly, feature interactions. While neural networks capture continuous user-related inputs such as timestamps and age to model temporal dynamics, the critical aspect lies in feature interactions. Feature interactions integrate latent representations from both continuous and categorical inputs, allowing the models to generate personalized recommendations. Non-sequential recommendation models focus solely on user activity to generate personalized recommendations, while sequential and session-based models, shown in Figure 1b, leverage users' historical interactions. Sequential and session-based models gain valuable insights into user preferences by considering the order and context of past actions, thereby enhancing recommendation accuracy.

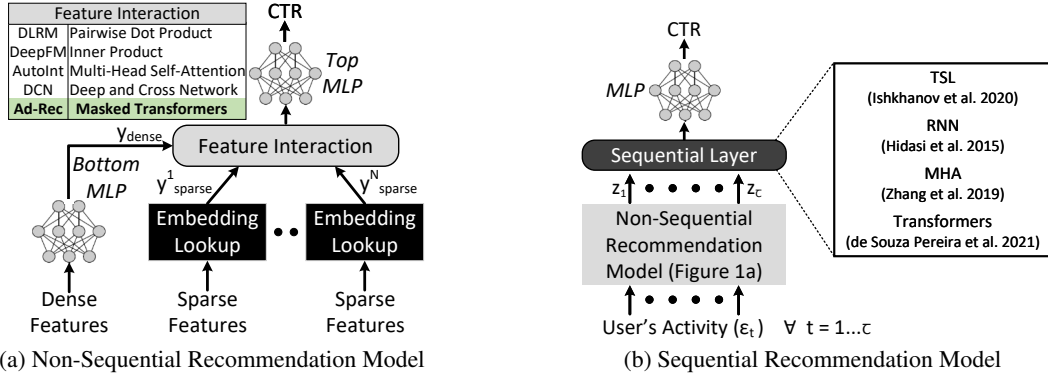


Figure 1: (a) Non-Sequential Deep Learning based Recommendation Model with multiple feature interaction techniques. (b) Sequential recommendation model with multiple sequential layers.

The feature interaction layer plays a crucial role in recommendation tasks by augmenting non-sequential and sequential models with valuable information beyond individual sparse and dense features [Naumov et al., 2019, Ishkhanov et al., 2020, Guo et al., 2017]. However, covariate shifts pose significant challenges for deep learning-based recommendation models. Manually identifying cross-features becomes impractical when dealing with a large number of features. This hinders model generalization. To overcome these challenges, deep neural network (DNN) based feature interaction techniques have emerged [Cheng et al., 2016, Guo et al., 2017, Lian et al., 2018, Shan et al., 2016, Song et al., 2019, Chen et al., 2019, Li et al., 2019]. These techniques allow for the extraction of higher-order features and effective generalization. However, including irrelevant feature interactions can introduce noise and lead to overfitting [Xiao et al., 2017, Zhu et al., 2021, Khawar et al., 2020, Liu et al., 2020, Su et al., 2021]. Moreover, modelling all feature interactions in the same space limits generality. Such an approach also fails to capture diverse patterns.

This paper proposes Ad-Rec, a masked transformer-based approach to address covariate shifts, eliminate irrelevant cross-features, and encompass various feature interaction patterns. Ad-Rec incorporates three key elements. First, it uses LayerNorm for mitigating internal covariate shifts. Second, it incorporates Multi-head Attention for modelling feature interactions in multiple subspaces, thereby enhancing generalization. Lastly, it employs Attention Masks to eliminate irrelevant cross-features in different subspaces. By stacking multiple transformer encoders, Ad-Rec effectively captures feature interactions at several (higher and lower) orders, enabling successful recommendations in the presence of covariate shifts.

We conduct experiments across various non-sequential and sequential models to evaluate Ad-Rec. On average, Ad-Rec achieves the desired AUC target in 58% training iterations compared to state-of-the-art DCN-v2 [Wang et al., 2021] model. This translates to training speedup of $1.4\times$ across seven different models and four real-world publically available datasets [CriteoLabs, a,b, Kaggle, Alibaba].

2 Related Work

1. Enhanced Models: Recommendation models are essential for delivering personalized user experiences by suggesting items based on the correlation between multiple input features. Approaches such as collaborative filtering (CF)[He et al., 2017] and matrix factorization (MF)[Koren et al., 2009, Weimer et al., 2007, Hidasi and Tikk, 2012] decompose user-item interactions into latent features. However, they have limitations in capturing complex feature interactions due to their reliance on linear combinations of latent features. Item-based neighbourhood methods offer an alternative for recommendation tasks [Sarwar et al., 2001, Koren, 2008].

Deep learning has revolutionized recommendation models, enabling more accurate capturing of intricate feature interactions. Models like Multi-Layer Perceptron (MLP)[Cheng et al., 2016, Zhao et al., 2019] and neural networks[Naumov et al., 2019] have shown promise in capturing and modelling complex feature relationships. Additionally, techniques such as autoencoders [Sedhain et al., 2015] and Gated Recurrent Units (GRU)[Hidasi et al., 2015] have been employed to account for temporal dependencies in user interactions. To address the temporal nature of user behaviour,

sequential recommendation models [Ishkhanov et al., 2020, Chen et al., 2019, Sun et al., 2019] have been developed, while session-based recommendation models focus on utilizing the user’s current session history [de Souza Pereira Moreira et al., 2021]. These existing methods still face challenges in effectively capturing and modelling the intricate relationships between features.

2. Learning Feature Interactions: Recommendation models have been extensively studied in the machine-learning community. Traditional approaches, such as collaborative filtering [He et al., 2017] and matrix factorization [Koren et al., 2009, Weimer et al., 2007, Hidasi and Tikk, 2012], have been widely used to decompose user-item interactions into latent features. Item-based neighbourhood methods [Sarwar et al., 2001, Koren, 2008] have also been employed for recommendation tasks. With the advent of deep learning, various models, including Multi-Layer Perceptron (MLP) [Cheng et al., 2016, Zhao et al., 2019], neural networks [Naumov et al., 2019], autoencoders [Sedhain et al., 2015], and Gated Recurrent Units (GRU) [Hidasi et al., 2015], have been proposed to capture more complex feature interactions and temporal dependencies in user interactions. Sequential recommendation models [Ishkhanov et al., 2020, Chen et al., 2019, Sun et al., 2019] and session-based recommendation models [de Souza Pereira Moreira et al., 2021] have also gained attention in capturing the temporal sequence of user behaviour. While these existing methods have made significant contributions to feature interaction modelling in recommendation systems, they primarily focus on lower-order interactions. They often struggle to capture higher-order feature interactions.

3. Eliminating Useless Features: Several existing methods have attempted to enhance feature interaction modelling in recommendation systems. AFM [Xiao et al., 2017] introduces the concept of distinguishing between different feature interactions, but it falls short in eliminating cross-features. AIM [Xiao et al., 2017] and AutoFIS [Liu et al., 2020] take a different approach by employing selection gating to prune irrelevant feature interactions. AutoFeature [Khawar et al., 2020] introduces a NAS-based approach to identify essential feature interactions. Unfortunately, these methods often focus on specific aspects of feature interactions and fail to provide a comprehensive solution.

3 Proposed Architecture: Ad-Rec

Ad-Rec utilizes a masked transformers-based approach (Figure 2a) to handle data drift, minimize noise from irrelevant cross-features, and capture diverse patterns for higher-order interactions. Transformers are renowned for their ability to learn sequential correlations and encode word sequences using token embeddings and positional encoding.

In addition, Ad-Rec incorporates a Bottom MLP (MLP_{bot}) to process dense inputs $\mathbf{x}_{\text{dense}}$, generating $\mathbf{y}_{\text{dense}}$ (Equation 1). Sparse inputs $\mathbf{x}_{\text{sparse}}$ undergo an embedding lookup using the embedding table $\mathbf{E} \in \mathbb{R}^{M \times D}$, producing $\mathbf{y}_{\text{sparse}}$ (Equation 2). Here, M represents the number of items in the feature embedding \mathbf{E} , and D denotes the sparse feature size.

$$\mathbf{y}_{\text{dense}} = \text{MLP}_{\text{bot}}(\mathbf{x}_{\text{dense}}) \tag{1}$$

$$\mathbf{y}_{\text{sparse}} = \mathbf{x}_{\text{sparse}}\mathbf{E} \quad \mathbf{E} \in \mathbb{R}^{M \times D} \tag{2}$$

The outputs of dense and sparse features are concatenated to form the feature sequence $\mathbf{z}_0 \in \mathbb{R}^{(N+1) \times D}$ (Equations 3 and 4). The feature sequence \mathbf{z}_0 captures joint embeddings of $N + 1$ input features, where each feature is associated with a latent vector of size D .

$$\mathbf{z}_0 = [\text{MLP}_{\text{bot}}(\mathbf{x}_{\text{dense}}); \mathbf{x}_{\text{sparse}}^1 \mathbf{E}^1; \dots; \mathbf{x}_{\text{sparse}}^N \mathbf{E}^N] \tag{3}$$

$$\mathbf{z}_0 = [\mathbf{y}_{\text{dense}}; \mathbf{y}_{\text{sparse}}^1; \dots; \mathbf{y}_{\text{sparse}}^N] \tag{4}$$

This design empowers Ad-Rec to model feature interactions across multiple dimensions, addressing the challenge of capturing diverse patterns for higher-order cross-features. In deep learning-based recommender systems, the feature sequence \mathbf{z}_0 is either used directly or dot-product-based feature interactions are computed as *lower triangle*($\mathbf{z}_0 \times \mathbf{z}_0^T$) to extract second-order cross-features.

3.1 Masked Attention

The core component of Ad-Rec is the masked multi-head attention block, which enables explicit cross-feature creation in multiple subspaces while eliminating irrelevant ones. Figure 2b visually demonstrates the masking process for removing irrelevant cross-features.

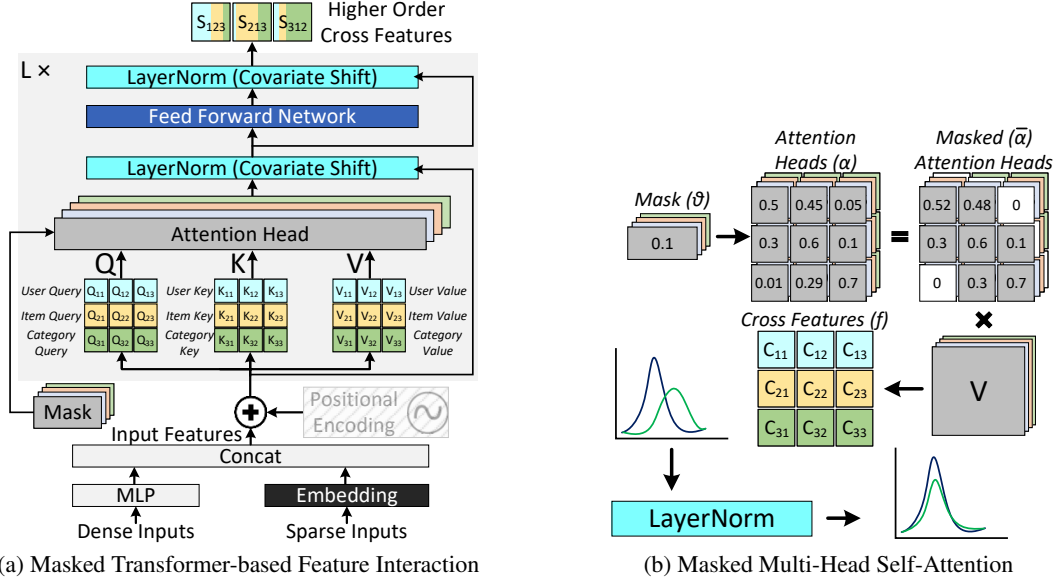


Figure 2: (a) The masked transformer-based feature interaction enables efficient higher-order cross-features by using embedding tables and masking to eliminate irrelevant cross-features. LayerNorm further enhances cross-feature quality. (b) In the masked multi-head self-attention mechanism, scalar masks are assigned to each head to eliminate irrelevant cross-features, allowing for diverse cross-feature patterns in multiple subspaces. LayerNorm reduces internal covariate shift, leading to faster convergence and improved learning.

Each input feature z_i has query and key-value pairs learned in h subspaces, corresponding to the number of attention heads. This allows for capturing diverse cross-features in multiple subspaces. This is achieved through linear projection using matrices W_Q^h , W_K^h , and $W_V^h \in \mathbb{R}^{D \times D'}$, where $D' = \frac{D}{h}$. Specifically, the projected query, key, and value vectors for feature i in subspace h are denoted as $z_{qi}^h = z_i W_Q^h$, $z_{ki}^h = z_i W_K^h$, and $z_{vi}^h = z_i W_V^h$, respectively. The correlation between feature i and feature j under a specific subspace h is represented by the attention head $\alpha_{i,j}^h$ (Equation 5), where $\langle \cdot \rangle$ denotes the inner product.

$$\alpha_{i,j}^h = \frac{\exp\langle z_{qi}^h \cdot z_{kj}^h \rangle}{\sum_{m=1}^{N+1} \exp\langle z_{qi}^h \cdot z_{km}^h \rangle} \quad (5)$$

Masking: Ad-Rec uses a masking technique to eliminate irrelevant feature interactions. Each head h has a mask θ . The masked attention score $\overline{\langle z_{qi}^h \cdot z_{kj}^h \rangle}$ is calculated as follows (Equation 6):

$$\overline{\langle z_{qi}^h \cdot z_{kj}^h \rangle} = \begin{cases} \langle z_{qi}^h \cdot z_{kj}^h \rangle, & \text{if } \alpha_{i,j}^h > \theta^h \\ -\infty, & \text{otherwise} \end{cases} \quad (6)$$

The recalculated attention head $\overline{\alpha}_{i,j}^h$ (Equation 7) is obtained by applying the softmax function to the masked attention scores:

$$\overline{\alpha}_{i,j}^h = \frac{\exp\overline{\langle z_{qi}^h \cdot z_{kj}^h \rangle}}{\sum_{m=1}^{N+1} \exp\overline{\langle z_{qi}^h \cdot z_{km}^h \rangle}} \quad (7)$$

Finally, the cross-feature of feature i in subspace h is updated by combining the relevant feature attentions $\overline{\alpha}_{i,j}^h$ with the corresponding values z_{vm}^h (Equation 8):

$$f_i^h = \sum_{m=1}^{N+1} \overline{\alpha}_{i,m}^h \cdot z_{vm}^h \quad (8)$$

θ^h is a head-specific mask that is fixed before training. In this work, a geometric sequence of decreasing values, such as $\frac{1}{10^1}, \frac{1}{10^2}, \dots, \frac{1}{10^h}$, was used for the masks of multiple heads. This choice eliminates irrelevant features. While a single mask could be used for all heads, different masks per head allow for generalization. Appendix A.3 presents an ablation study on different mask values.

LayerNorm: Ad-Rec utilizes Layer Normalization (LayerNorm) to normalize the output of the masked attention layer and feedforward network, ensuring stable and efficient training.

LayerNorm (LN), when applied to \mathbf{f}_i^h of the masked attention layer, is defined using Equation 9.

$$\overline{\mathbf{f}}_i^h = \text{LN}(\mathbf{f}_i^h) = \frac{\mathbf{f}_i^h - \mu_i^h}{\sqrt{\sigma_i^2 + \epsilon}} \odot \gamma^h + \beta^h \quad (9)$$

Here, μ_i^h and σ_i^2 are the mean and variance of \mathbf{f}_i^h across feature dimensions, respectively. The \odot operator represents element-wise multiplication. The learnable parameters γ^h and β^h scale and shift the normalized values. The term ϵ ensures numerical stability.

LayerNorm normalizes the output of the masked attention layer, \mathbf{f}_i^h , to have zero mean and unit variance across feature dimensions. This mitigates covariate shifts and provides a stable distribution for subsequent layers. The scale and shift parameters, γ^h and β^h , enable the model to capture appropriate representations for the recommendation task.

LayerNorm also has a similar effect on the output of the feedforward network. By reducing reliance on the scale and distribution of the training dataset, it facilitates faster convergence, offers modest regularization, and improves the efficiency of parameter updates in the recommendation model.

Positional Embedding: While positional embeddings are commonly used in language tasks to preserve word order, they are not utilized in Ad-Rec for recommender systems. Despite this, we evaluated 1-D positional embeddings to encode spatial information of features. The findings in Appendix A.4 indicate that including positional embedding adversely affects the model’s performance.

Ad-Rec employs masked multi-head attention (MSA) to learn explicit higher-order cross-features in multiple subspaces, and the feedforward network (FFN) handles implicit interactions. By stacking multiple Ad-Rec layers, up to L (Equations 10 and 11), higher-order interactions can be captured more effectively (see Appendix A.5.1). It also improves performance for larger input feature sequences.

$$\mathbf{z}'_\ell = \text{Masked MSA}(\text{LN}(\mathbf{z}_{\ell-1})) + \mathbf{z}_{\ell-1}, \quad \ell = 1, \dots, \mathbf{L} \quad (10)$$

$$\mathbf{z}_\ell = \text{FFN}(\text{LN}(\mathbf{z}'_\ell)) + \mathbf{z}_\ell, \quad \ell = 1, \dots, \mathbf{L} \quad (11)$$

The last layer’s output is concatenated with processed dense inputs, resulting in \mathbf{z} (Equation 12).

$$\mathbf{z} = [\mathbf{y}_{\text{dense}}; \mathbf{z}_\ell] \quad (12)$$

The final click-through rate (CTR) is obtained by applying the top MLP (MLP_{top}) to \mathbf{z} (Equation 13). Thus, the problem is modelled as binary classification using binary cross-entropy (BCE) loss to predict whether a user will click the target item.

$$\text{CTR} = \text{MLP}_{\text{top}}(\mathbf{z}) \quad (13)$$

3.2 Application to Sequential Recommendation Models

For sequential recommendation models, we apply Ad-Rec by generating an embedding vector \mathbf{z}_t for each event ε_t using the non-sequential recommendation model. Here, ε_t represents the event at time step t , such as a user click or purchase. These embeddings capture event characteristics, including explicit timing as a dense feature. The width of the last layer in the non-sequential model is adjusted to match the user-interaction vector’s width, which is then fed into the sequential layer. This produces a sequence of embedding vectors Z (Equation 15).

$$\mathbf{z}_t = \text{AdRec}(\varepsilon_t) \quad t = 1, \dots, \tau \quad (14)$$

$$Z = [\mathbf{z}_1, \mathbf{z}_2, \dots, \mathbf{z}_{\tau-1}] \quad (15)$$

$$\mathbf{c} = \text{SequentialLayer}(\mathbf{z}_\tau, Z) \quad (16)$$

Ad-Rec generates an embedding \mathbf{z}_t for each event, capturing relevant information about the user-item interaction. These embeddings are used as input to the sequential layer, which considers the context and temporal order of earlier events to predict the next event ε_τ at time step τ (Equation 16). By leveraging the Ad-Rec embeddings, the model effectively captures user-item interactions within the sequence, leading to improved recommendation performance.

4 Ad-Rec Analysis

To analyze the feature interaction of DLRM and Ad-Rec, we randomly sampled a test input from the real-world Taobao user behaviour dataset [Alibaba]. This input consists of sequential user activity with a length of 21, a timestamp as a dense feature, and sparse features for user, item, and category. Notably, the ground truth of the sampled input indicates that it is a **negative sample**.

Figure 3 presents the cosine similarity heat map, comparing the feature interaction of DLRM and Ad-Rec. In DLRM, the feature interaction is based on dot product calculations, while Ad-Rec employs masked attention. The features involved in the interaction include the user’s activity timestamp (feature 1), user ID (feature 2), item ID (feature 3), and item category (feature 4).

Examining the sequential interaction at timestamp $t = 2$ in Figure 3, we observe contrasting behaviour between DLRM and Ad-Rec. We observe that DLRM’s dot product-based feature interaction provides close similarity across all pairs. Contrary to this, Ad-Rec’s masked attention-based feature interaction considers Query (**Q**) and Key (**K**) projections. Applying a mask with $\frac{1}{10^3}$ value reveals no features being masked (note that the mappings of attention heads can be found in Appendix A.6).

The highest weight is assigned to feature pair (2, 3), indicating a strong correlation between user ID and item ID. In contrast, other pairs such as (1, 2), (1, 4), (2, 4), and (3, 4) show weak alignment, implying a primarily **negative sample**. Unlike DLRM’s dot product-based feature interaction, Ad-Rec captures this information.

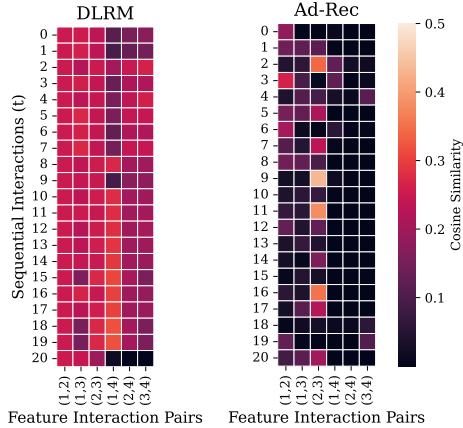


Figure 3: Cosine similarity of feature interaction in the real-world Taobao dataset: one dense and three sparse features for a single user.

5 Experiments and Results

5.1 Evaluation Setup

Recommendation Models: We train recommendation models with varying sizes to represent different classes of at-scale models [Gupta et al., 2020, Adnan et al., 2022a,b]. The architecture of these models is presented in Table 1 [Wu et al., 2019, Zhao et al., 2019].

These models are selected based on their diverse characteristics and parameter sizes. The sparse parameter count ranges from 5.2M (RM4) to 266M (RM2), indicating different model complexity and capacity levels. It is worth noting that RM1 and RM2 are embedding-dominated models. On the other hand, RM3 is an average-sized model with a balanced mix of dense and sparse features.

To further explore the impact of sequential information, we consider models RM4, RM5, RM6, and RM7, which share a common base model for generating embedding vectors per event. However, they differ in the choice of the sequential layer to process the temporal sequence. RM4 employs a single time series layer (TSL), RM5 utilizes multi-head attention with eight heads, RM6 consists of 5 RNN layers, and RM7 employs a single transformer layer to predict the probability of the next event.

Datasets: We investigate Ad-Rec’s performance using various real-world datasets for both non-sequential and sequential recommendation tasks. For non-sequential tasks, we employ three datasets:

Table 1: Recommendation Models Architecture and Ad-Rec Configuration (# layers = 1)

Model	Dataset	Features		Parameters			Neural Network Configuration		Ad-Rec Configuration			Sequential Layer	
		Dense	Sparse	Dense	Sparse	Sparse Dim	Bottom MLP	Top MLP	Num Heads	Hidden Size	FFN Config.	Type	Layers/ Heads
RM1	Criteo Kaggle	13	26	287.5k	33.8M	16	13-512-256-64-16	512-256-1	2	16	128	N/A	N/A
RM2	Criteo Terabyte	13	26	549.1k	266M	64	13-512-256-64	512-512-256-1	8	64	512	N/A	N/A
RM3	Avazu	1	21	281.4k	9.3M	16	1-512-256-64-16	512-256-1	2	16	128	N/A	N/A
RM4	Taobao Alibaba	1	3	7.3k	5.1M	16	1-16	22-15-15	2	16	128	TSL	1
RM5												MHA	8
RM6												RNN	5
RM7												Transformer	1

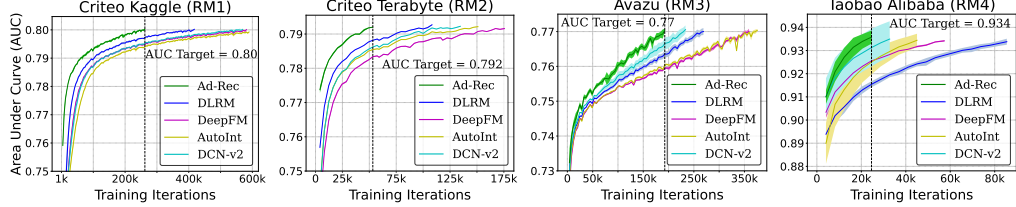


Figure 4: Comparison of Ad-Rec’s convergence with baseline feature interaction techniques. The dotted vertical line represents the training iteration where Ad-Rec reaches the target AUC and stops training. On average, Ad-Rec achieves target AUC in 50%, 42%, 45%, and 58% lower iterations, as compared to the DLRM, DeepFM, AutoInt, and DCN-v2 baselines.

Criteo Kaggle [CriteoLabs, a], Criteo Terabyte [CriteoLabs, b], and Avazu [Kaggle]. The Criteo Kaggle dataset, derived from the Display Advertising Challenge, predicts click-through rates (CTR) and captures user preferences. Criteo Terabyte, the largest publicly available click-log dataset, is commonly used to train non-sequential DLRM models. The Avazu dataset, obtained from a CTR prediction competition on Kaggle, provides insights into users’ ad click behaviours for mobile ads.

For sequential recommendation models, we turn to the Taobao User Behavior dataset [Alibaba], encompassing a vast array of 4 million items, 10,000 categories, and 1 million users. Within this dataset, each user’s time series comprises triplets (i, c, t) , representing the interactions where a user u engages with an item i from category c at time t . With an average of 21 sequential interaction events per user, the Taobao User Behavior dataset offers a rich environment to evaluate Ad-Rec.

Baselines: We compare Ad-Rec against four state-of-the-art techniques. DLRM [Naumov et al., 2019] and DeepFM [Guo et al., 2017] are 2nd order feature interaction while AutoInt [Song et al., 2019] and DCN-v2 [Wang et al., 2021] are higher-order feature interaction techniques.

Training Details: We conducted our experiments using PyTorch-1.9 and built upon the widely adopted Deep Learning Recommendation Model (DLRM) [Naumov et al., 2019] for non-sequential recommendations and Time-Based Sequence Model (TBSM) [Ishkhanov et al., 2020] for the sequential counterpart. All models were implemented identically to ensure a fair comparison, with the feature interaction component being the only point of distinction.

For non-sequential models (RM1, RM2, and RM3), we employed the Stochastic Gradient Descent (SGD) [Bottou, 2012] optimizer. RM1 and RM3 were trained with a batch size of 128, while RM2 utilized a batch size of 1024. The learning rates were set to 0.01 for RM1, 0.1 for RM2, and 0.2 for RM3. In the case of sequential models (RM4, RM5, RM6, and RM7), we employed the Adagrad [Duchi et al., 2011] optimizer with a learning rate of 0.05 and a batch size of 128.

We performed five independent runs and presented the mean and standard deviation of the results. All models, except RM2, were trained on a single NVIDIA Tesla-V100 GPU. Due to the size of its embedding tables, RM2 was trained on 4 NVIDIA Tesla-V100 GPUs to ensure proper fitting.

Evaluation Metrics: For evaluating the performance of our recommendation models, we use the Area Under Curve (AUC) metric, as established by the MLPerf community [MLCommons]. The AUC metric measures the probability that a randomly selected positive sample will be ranked higher than a randomly chosen negative sample. A higher AUC score indicates better performance. Each model is trained to achieve a specific target AUC score. Even a slight improvement in AUC, such as 0.001, is considered significant for click-through rate (CTR) prediction [Cheng et al., 2016, Guo et al., 2017, Li et al., 2019]. We also track testing accuracy and BCE loss along with the AUC metric.

5.2 Convergence Analysis

We compare the convergence of Ad-Rec with the baseline models (RM1, RM2, RM3, and RM4) by setting a target AUC for each model based on prior work Naumov et al. [2019], Ishkhanov et al. [2020]. The baseline models and Ad-Rec are trained with early stopping to achieve the target AUC. Figure 4 demonstrates that Ad-Rec achieves the target AUC in fewer training iterations, thanks to its masked attention-based feature interaction. The transformer encoder in Ad-Rec captures the relationships between input features, resulting in deeper feature representations and improved learning and prediction. On average, Ad-Rec achieves the target AUC in 50%, 42%, 45%, and 58% iterations, surpassing the DLRM, DeepFM, AutoInt, and DCN-v2 baselines.

Table 2 compares evaluation metrics for a single training epoch. Across all models and datasets, Ad-Rec consistently outperforms the baselines regarding AUC. On average, Ad-Rec improves the AUC metric by 0.012, 0.008, 0.006, and 0.001 compared to the DLRM, DeepFM, AutoInt, and DCN-v2 baselines. Although higher-order feature interaction techniques may exhibit lower performance in certain models and datasets, Ad-Rec showcases superior generalization capabilities. It consistently outperforms other feature interaction techniques. For a comprehensive analysis of Ad-Rec’s hyperparameters, please refer to the ablation study in Appendix A.5.

Table 2: Evaluation Metric Comparison with Single Epoch Training - Mean (stddev)

Model	AUC					BCE Loss				
	DLRM	DeepFM	AutoInt	DCN-v2	Ad-Rec	DLRM	DeepFM	AutoInt	DCN-v2	Ad-Rec
RM1	0.798 (1.9e-4)	0.796 (1.6e-4)	0.795 (8.12e-5)	0.796 (2.9e-4)	0.801 (1e-4)	0.459 (1.5e-3)	0.461 (1.6e-3)	0.461 (1.4e-3)	0.460 (1.3e-3)	0.455 (1.4e-3)
RM2	0.788 (1.8e-4)	0.783 (1.5e-4)	0.785 (1.5e-4)	0.786 (8.29e-5)	0.790 (1.8e-4)	0.424 (1.4e-4)	0.428 (1.5e-4)	0.426 (7.25e-5)	0.426 (5.14e-5)	0.423 (9.4e-5)
RM3	0.768 (9.5e-4)	0.763 (3.4e-3)	0.763 (7.8e-4)	0.772 (1e-3)	0.775 (3.2e-4)	0.386 (3.8e-4)	0.390 (2.6e-4)	0.390 (3.6e-4)	0.384 (5e-4)	0.382 (1.2e-4)
RM4	0.933 (1.3e-4)	0.939 (6.6e-4)	0.942 (1.5e-3)	0.947 (5.8e-3)	0.949 (1.9e-3)	0.267 (3.4e-3)	0.257 (1.3e-3)	0.254 (3.8e-3)	0.237 (1.5e-2)	0.232 (8.3e-3)
RM5	0.869 (4.2e-4)	0.881 (1.1e-4)	0.893 (5.5e-3)	0.894 (1.5e-3)	0.895 (2.1e-3)	0.378 (1.8e-4)	0.360 (6.3e-3)	0.363 (1.9e-3)	0.361 (3.2e-3)	0.361 (2e-3)
RM6	0.840 (7.1e-3)	0.850 (1e-3)	0.849 (2.8e-3)	0.855 (1.3e-3)	0.852 (2.6e-3)	0.385 (1.4e-3)	0.388 (3.7e-3)	0.388 (7.2e-3)	0.375 (1.1e-3)	0.380 (4.2e-3)
RM7	0.920 (1.8e-3)	0.934 (1.3e-3)	0.932 (6e-3)	0.940 (5.2e-3)	0.940 (1.8e-3)	0.299 (1.1e-3)	0.269 (2.8e-3)	0.279 (1.2e-3)	0.255 (1.3e-3)	0.254 (5.6e-3)

Performance Comparison: Ad-Rec’s transformer-based feature interaction is computationally expensive compared to baselines. The wall clock time is measured to compare the runtime of training the recommendation model. As Figure 5 shows, as expected, a single training iteration of Ad-Rec-based training takes more time. Still, it converges in less number of training iterations that provides a speedup of 1.5×, 2×, 2.1× and 1.4× over DLRM, DeepFM, AutoInt, and DCN-v2 baselines.

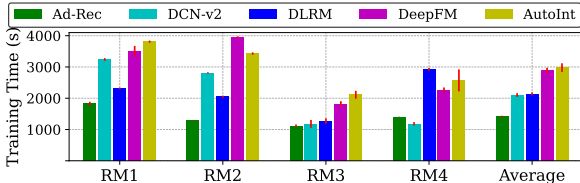


Figure 5: Absolute training time over multiple runs. Ad-Rec converges to target AUC in less time, which translates to a speedup of 1.5×, 2×, 2.1× and 1.4× over DLRM, DeepFM, AutoInt, and DCN-v2 baselines.

Computational Cost Analysis: To compare the computational cost of Ad-Rec-based feature interaction, we trained DLRM and Ad-Rec using a fixed computational budget and compared the training quality metric (AUC). Figure 6 shows that Ad-Rec dominates DLRM on this performance-compute trade-off. Similar trends are observed for other remaining models (RM2 and RM4).

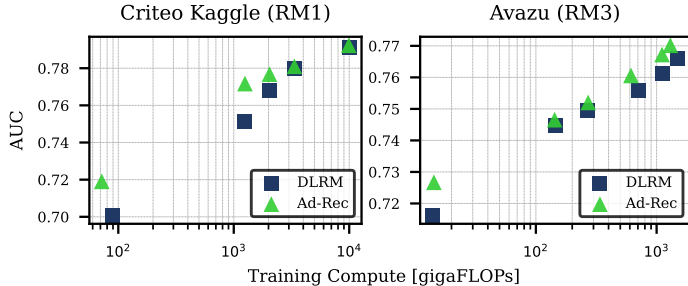


Figure 6: Model quality versus computational cost for different models. Ad-Rec outperforms state-of-the-art DLRM with the same computational budget.

5.3 Ablation Study for Covariate Shift

We evaluate the importance of LayerNorm in Ad-Rec with an ablation study that removes the LayerNorm layer while keeping the rest of the architecture unchanged. Table 3 shows a decrease in the AUC metric and an increase in the BCE Loss when LayerNorm is omitted. Thus LayerNorm is critical to handling data distribution drift and promoting faster and more stable convergence in Ad-Rec.

Table 3: Ablation study comparing the impact of LayerNorm (LN) in Ad-Rec to handle covariate shift.

Model	AUC		BCE Loss	
	Ad-Rec w/ LN	Ad-Rec w/o LN	Ad-Rec w/ LN	Ad-Rec w/o LN
RM1	0.801 (1e-4)	0.795 (2.4e-4)	0.455 (1.4e-3)	0.460 (1.4e-3)
RM2	0.790 (1.8e-4)	0.785 (2.2e-4)	0.423 (9.4e-5)	0.426 (1.4e-4)
RM3	0.775 (3.2e-4)	0.771 (1.8e-4)	0.382 (1.2e-4)	0.385 (1.4e-4)
RM4	0.949 (1.9e-3)	0.944 (2.8e-3)	0.232 (8.3e-3)	0.247 (7.4e-3)
RM5	0.895 (2.1e-3)	0.890 (2.8e-3)	0.361 (2e-3)	0.366 (5.9e-3)
RM6	0.852 (2.6e-3)	0.823 (7.3e-3)	0.400 (4.2e-4)	0.427 (6.3e-3)
RM7	0.940 (1.8e-3)	0.930 (2e-3)	0.272 (5.6e-3)	0.284 (4.8e-3)

5.4 Scaling the Recommendation Models

We conducted scaling ablation studies on DLRM-style recommendation models. Scaling the embedding dimension had the most significant improvement, while scaling the model size had minimal effect on model quality. More details can be found in Appendix A.7. In the ablation studies with Ad-Rec, we evaluated model quality using masked-attention-based feature interaction while keeping the model size and computational budget fixed. Figure 7 shows that Ad-Rec consistently outperformed other models across parameters, such as embeddings, embedding dimension, and neural network size.

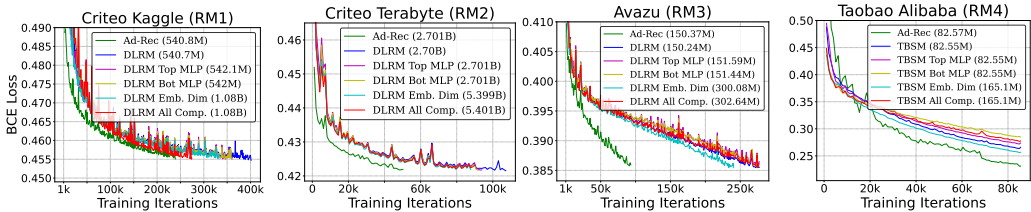


Figure 7: Scaling laws of recommendation models were studied to understand the impact of component scaling on model quality. Despite a small training dataset, Ad-Rec outperformed scaled models.

6 Limitations and Future Work

While Ad-Rec exhibits promising results, two key areas warrant further investigation. First, the masked attention-based feature interaction in Ad-Rec enhances model performance but may compromise interpretability compared to other techniques. Future work can focus on developing approaches to improve inter-operability. Second, recent higher-order feature interaction techniques, including Ad-Rec and AutoInt [Song et al., 2019], exhibit increased inference time due to their higher computational complexity for attention-based operations. Meeting strict Service Level Agreements (SLAs) becomes challenging with such higher-order techniques. Future research could explore leveraging the learned features from Ad-Rec and applying less computationally expensive feature interaction techniques.

7 Conclusion

Recommendation models are pivotal in improving recommendation quality and user experience, attracting considerable attention from industry and academia. In this study, we tackled the challenges of covariate shifts and sought to enhance cross-feature learning while accounting for data drift. Our findings underscored the significance of normalizing explicit cross-features and eliminating noisy ones to enhance recommendations in unfamiliar data distributions. To address these challenges, we introduced Ad-Rec, a masked-attention-based feature interaction technique. Through rigorous experimentation, Ad-Rec consistently outperformed state-of-the-art baselines, exhibiting superior quality and convergence speed. It achieved higher AUC scores and accelerated the training process, delivering compelling results across commercial models and publicly available datasets.

References

- Muhammad Adnan, Yassaman Ebrahimzadeh Maboud, Divya Mahajan, and Prashant J. Nair. Accelerating recommendation system training by leveraging popular choices. *Proc. VLDB Endow.*, 15(1):127–140, jan 2022a. ISSN 2150-8097. doi: 10.14778/3485450.3485462. URL <https://doi.org/10.14778/3485450.3485462>.
- Muhammad Adnan, Yassaman Ebrahimzadeh Maboud, Divya Mahajan, and Prashant J. Nair. Heterogeneous acceleration pipeline for recommendation system training, 2022b.
- Alibaba. User behavior data from taobao for recommendation. <https://tianchi.aliyun.com/dataset/dataDetail?dataId=649&userId=1>.
- Newsha Ardalani, Carole-Jean Wu, Zeliang Chen, Bhargav Bhushanam, and Adnan Aziz. Understanding scaling laws for recommendation models, 2022. URL <https://arxiv.org/abs/2208.08489>.
- Léon Bottou. Stochastic gradient descent tricks. In *Neural networks: Tricks of the trade*, pages 421–436. Springer, 2012.
- Qiwei Chen, Huan Zhao, Wei Li, Pipei Huang, and Wenwu Ou. Behavior sequence transformer for e-commerce recommendation in alibaba. In *Proceedings of the 1st International Workshop on Deep Learning Practice for High-Dimensional Sparse Data, DLP-KDD '19*, New York, NY, USA, 2019. Association for Computing Machinery. ISBN 9781450367837. doi: 10.1145/3326937.3341261. URL <https://doi.org/10.1145/3326937.3341261>.
- Heng-Tze Cheng, Levent Koc, Jeremiah Harmsen, Tal Shaked, Tushar Chandra, Hrishu Aradhye, Glen Anderson, Greg Corrado, Wei Chai, Mustafa Ispir, Rohan Anil, Zakaria Haque, Lichan Hong, Vihan Jain, Xiaobing Liu, and Hemal Shah. Wide and deep learning for recommender systems. In *Proceedings of the 1st Workshop on Deep Learning for Recommender Systems, DLRS 2016*, page 7–10, New York, NY, USA, 2016. Association for Computing Machinery. ISBN 9781450347952. doi: 10.1145/2988450.2988454. URL <https://doi.org/10.1145/2988450.2988454>.
- CriteoLabs. Criteo display ad challenge, a. <https://www.kaggle.com/c/criteo-display-ad-challenge>.
- CriteoLabs. Terabyte click logs, b. <https://labs.criteo.com/2013/12/download-terabyte-click-logs>.
- Gabriel de Souza Pereira Moreira, Sara Rabhi, Jeong Min Lee, Ronay Ak, and Even Oldridge. Transformers4rec: Bridging the gap between nlp and sequential / session-based recommendation. In *Proceedings of the 15th ACM Conference on Recommender Systems, RecSys '21*, page 143–153, New York, NY, USA, 2021. Association for Computing Machinery. ISBN 9781450384582. doi: 10.1145/3460231.3474255. URL <https://doi.org/10.1145/3460231.3474255>.
- John Duchi, Elad Hazan, and Yoram Singer. Adaptive subgradient methods for online learning and stochastic optimization. *Journal of machine learning research*, 12(7), 2011.
- Huifeng Guo, Ruiming Tang, Yunming Ye, Zhenguo Li, and Xiuqiang He. Deepfm: a factorization-machine based neural network for ctr prediction. *arXiv preprint arXiv:1703.04247*, 2017.
- U. Gupta, C. Wu, X. Wang, M. Naumov, B. Reagen, D. Brooks, B. Cotel, K. Hazelwood, M. Hempstead, B. Jia, H. S. Lee, A. Malevich, D. Mudigere, M. Smelyanskiy, L. Xiong, and X. Zhang. The architectural implications of facebook’s dnn-based personalized recommendation. In *2020 IEEE International Symposium on High Performance Computer Architecture (HPCA)*, pages 488–501, 2020. doi: 10.1109/HPCA47549.2020.00047.
- Xiangnan He, Lizi Liao, Hanwang Zhang, Liqiang Nie, Xia Hu, and Tat-Seng Chua. Neural collaborative filtering. In *Proceedings of the 26th International Conference on World Wide Web, WWW '17*, page 173–182, Republic and Canton of Geneva, CHE, 2017. International World Wide Web Conferences Steering Committee. ISBN 9781450349130. doi: 10.1145/3038912.3052569. URL <https://doi.org/10.1145/3038912.3052569>.

- Balázs Hidasi and Domonkos Tikk. Fast als-based tensor factorization for context-aware recommendation from implicit feedback. In *Proceedings of the 2012th European Conference on Machine Learning and Knowledge Discovery in Databases - Volume Part II, ECMLPKDD'12*, page 67–82, Berlin, Heidelberg, 2012. Springer-Verlag. ISBN 9783642334856.
- Balázs Hidasi, Alexandros Karatzoglou, Linas Baltrunas, and Domonkos Tikk. Session-based recommendations with recurrent neural networks. *arXiv preprint arXiv:1511.06939*, 2015.
- T. Ishkhanov, M. Naumov, X. Chen, Y. Zhu, Y. Zhong, A. G. Azzolini, C. Sun, F. Jiang, A. Malevich, and L. Xiong. Time-based sequence model for personalization and recommendation systems. *CoRR*, abs/2008.11922, 2020. URL <https://arxiv.org/abs/2008.11922>.
- Kaggle. Avazu mobile ads ctr. <https://www.kaggle.com/c/avazu-ctr-prediction>.
- Farhan Khawar, Xu Hang, Ruiming Tang, Bin Liu, Zhenguo Li, and Xiuqiang He. Autofeature: Searching for feature interactions and their architectures for click-through rate prediction. In *Proceedings of the 29th ACM International Conference on Information & Knowledge Management*, pages 625–634, 2020.
- Y. Koren, R. Bell, and C. Volinsky. Matrix factorization techniques for recommender systems. *Computer*, 42(8):30–37, 2009. doi: 10.1109/MC.2009.263.
- Yehuda Koren. Factorization meets the neighborhood: A multifaceted collaborative filtering model. In *Proceedings of the 14th ACM SIGKDD International Conference on Knowledge Discovery and Data Mining, KDD '08*, page 426–434, New York, NY, USA, 2008. Association for Computing Machinery. ISBN 9781605581934. doi: 10.1145/1401890.1401944. URL <https://doi.org/10.1145/1401890.1401944>.
- Zekun Li, Zeyu Cui, Shu Wu, Xiaoyu Zhang, and Liang Wang. Fi-gnn: Modeling feature interactions via graph neural networks for ctr prediction. In *Proceedings of the 28th ACM International Conference on Information and Knowledge Management*, pages 539–548, 2019.
- Jianxun Lian, Xiaohuan Zhou, Fuzheng Zhang, Zhongxia Chen, Xing Xie, and Guangzhong Sun. Xdeepfm: Combining explicit and implicit feature interactions for recommender systems. In *Proceedings of the 24th ACM SIGKDD International Conference on Knowledge Discovery and Data Mining, KDD '18*, page 1754–1763, New York, NY, USA, 2018. Association for Computing Machinery. ISBN 9781450355520. doi: 10.1145/3219819.3220023. URL <https://doi.org/10.1145/3219819.3220023>.
- Bin Liu, Chenxu Zhu, Guilin Li, Weinan Zhang, Jincan Lai, Ruiming Tang, Xiuqiang He, Zhenguo Li, and Yong Yu. Autofis: Automatic feature interaction selection in factorization models for click-through rate prediction. In *Proceedings of the 26th ACM SIGKDD International Conference on Knowledge Discovery & Data Mining*, pages 2636–2645, 2020.
- MLCommons. Mlperf benchmarks. <https://mlcommons.org/en/training-normal-10/>.
- Maxim Naumov, Dheevatsa Mudigere, Hao-Jun Michael Shi, Jianyu Huang, Narayanan Sundaraman, Jongsoo Park, Xiaodong Wang, Udit Gupta, Carole-Jean Wu, Alisson G. Azzolini, Dmytro Dzhulgakov, Andrey Mallevich, Ilia Cherniavskii, Yinghai Lu, Raghuraman Krishnamoorthi, Ansha Yu, Volodymyr Kondratenko, Stephanie Pereira, Xianjie Chen, Wenlin Chen, Vijay Rao, Bill Jia, Liang Xiong, and Misha Smelyanskiy. Deep learning recommendation model for personalization and recommendation systems. *CoRR*, abs/1906.00091, 2019. URL <https://arxiv.org/abs/1906.00091>.
- Badrul Sarwar, George Karypis, Joseph Konstan, and John Riedl. Item-based collaborative filtering recommendation algorithms. In *Proceedings of the 10th International Conference on World Wide Web, WWW '01*, page 285–295, New York, NY, USA, 2001. Association for Computing Machinery. ISBN 1581133480. doi: 10.1145/371920.372071. URL <https://doi.org/10.1145/371920.372071>.
- Suvash Sedhain, Aditya Krishna Menon, Scott Sanner, and Lexing Xie. Autorec: Autoencoders meet collaborative filtering. In *Proceedings of the 24th International Conference on World Wide Web, WWW '15 Companion*, page 111–112, New York, NY, USA, 2015. Association

- for Computing Machinery. ISBN 9781450334730. doi: 10.1145/2740908.2742726. URL <https://doi.org/10.1145/2740908.2742726>.
- Ying Shan, T. Ryan Hoens, Jian Jiao, Haijing Wang, Dong Yu, and JC Mao. Deep crossing: Web-scale modeling without manually crafted combinatorial features. In *Proceedings of the 22nd ACM SIGKDD International Conference on Knowledge Discovery and Data Mining*, KDD '16, page 255–262, New York, NY, USA, 2016. Association for Computing Machinery. ISBN 9781450342322. doi: 10.1145/2939672.2939704. URL <https://doi.org/10.1145/2939672.2939704>.
- Weiping Song, Chence Shi, Zhiping Xiao, Zhijian Duan, Yewen Xu, Ming Zhang, and Jian Tang. Autoint: Automatic feature interaction learning via self-attentive neural networks. In *Proceedings of the 28th ACM International Conference on Information and Knowledge Management*, pages 1161–1170, 2019.
- Yixin Su, Rui Zhang, Sarah Erfani, and Zhenghua Xu. Detecting beneficial feature interactions for recommender systems. In *Proceedings of the AAAI conference on artificial intelligence*, volume 35, pages 4357–4365, 2021.
- Fei Sun, Jun Liu, Jian Wu, Changhua Pei, Xiao Lin, Wenwu Ou, and Peng Jiang. Bert4rec: Sequential recommendation with bidirectional encoder representations from transformer. In *Proceedings of the 28th ACM international conference on information and knowledge management*, pages 1441–1450, 2019.
- Ruoxi Wang, Rakesh Shivanna, Derek Cheng, Sagar Jain, Dong Lin, Lichan Hong, and Ed Chi. Dcn v2: Improved deep & cross network and practical lessons for web-scale learning to rank systems. In *Proceedings of the web conference 2021*, pages 1785–1797, 2021.
- Markus Weimer, Alexandros Karatzoglou, Quoc Le, and Alex Smola. Cofi rank - maximum margin matrix factorization for collaborative ranking. In J. Platt, D. Koller, Y. Singer, and S. Roweis, editors, *Advances in Neural Information Processing Systems*, volume 20. Curran Associates, Inc., 2007. URL <https://proceedings.neurips.cc/paper/2007/file/f76a89f0cb91bc419542ce9fa43902dc-Paper.pdf>.
- C. Wu, D. Brooks, K. Chen, D. Chen, S. Choudhury, M. Dukhan, K. Hazelwood, E. Isaac, Y. Jia, B. Jia, T. Leyvand, H. Lu, Y. Lu, L. Qiao, B. Reagen, J. Spisak, F. Sun, A. Tulloch, P. Vajda, X. Wang, Y. Wang, B. Wasti, Y. Wu, R. Xian, S. Yoo, and P. Zhang. Machine learning at facebook: Understanding inference at the edge. In *2019 IEEE International Symposium on High Performance Computer Architecture (HPCA)*, pages 331–344, Feb 2019. doi: 10.1109/HPCA.2019.00048.
- Jun Xiao, Hao Ye, Xiangnan He, Hanwang Zhang, Fei Wu, and Tat-Seng Chua. Attentional factorization machines: Learning the weight of feature interactions via attention networks. *arXiv preprint arXiv:1708.04617*, 2017.
- Zhe Zhao, Lichan Hong, Li Wei, Jilin Chen, Aniruddh Nath, Shawn Andrews, Aditee Kumthekar, Maheswaran Sathiamoorthy, Xinyang Yi, and Ed Chi. Recommending what video to watch next: A multitask ranking system. In *Proceedings of the 13th ACM Conference on Recommender Systems*, RecSys '19, page 43–51, New York, NY, USA, 2019. Association for Computing Machinery. ISBN 9781450362436. doi: 10.1145/3298689.3346997. URL <https://doi.org/10.1145/3298689.3346997>.
- Chenxu Zhu, Bo Chen, Weinan Zhang, Jincal Lai, Ruiming Tang, Xiuqiang He, Zhenguo Li, and Yong Yu. Aim: Automatic interaction machine for click-through rate prediction. *IEEE Transactions on Knowledge and Data Engineering*, 2021.

A Appendix

A.1 High-Level Overview: Deep Learning-based Recommendations with Ad-Rec

Figure 1a illustrates the model architecture of Ad-Rec, a non-sequential deep learning-based recommendation model inspired by DLRM [Naumov et al., 2019]. The model takes two types of inputs: dense and sparse features. Dense inputs consist of continuous features such as the user’s age or the time of day. In contrast, sparse inputs include categorical features like the user’s location or liked videos.

Multi-layer perceptrons (MLPs) are employed to process the dense inputs, while large embedding tables handle the sparse inputs, each representing a specific categorical feature. These embeddings, along with the dense features, are then passed through a feature interaction layer, enabling the generation of cross-features that capture complex relationships between different features. Next, the cross-features and dense features are fed into an MLP layer, which predicts the click-through rate (CTR). The CTR indicates the likelihood of a user clicking on an item, serving as a key metric for recommendation models. By leveraging the power of deep learning and effective feature interaction, Ad-Rec enhances the accuracy and performance of recommendation systems.

Figure 1b provides an overview of sequential recommendation models within the context of Ad-Rec. These models explicitly incorporate the temporal aspect of user-item interactions through a set of events denoted as ε . Each event ε represents a user u interacting with an item i at a specific time t .

User behaviour is captured as a sequence of events ε spanning multiple time steps, denoted as $t = \{1, \dots, \tau - 1\}$. The sequential recommendation model is then trained to predict the next event at time step τ , based on the previous event sequence. This shift towards sequential modelling transforms the organization of the training dataset, as it now represents a sequence of user activities rather than a simple collection of user interactions with features, as seen in non-sequential recommendation models. By incorporating temporal dynamics, Ad-Rec enables more accurate and personalized recommendations in dynamic user environments.

A.2 Multihead Self-Attention

The standard self-attention mechanism, commonly used in Natural Language Processing (NLP) tasks, forms a fundamental building block. Given an input sequence $\mathbf{z} \in \mathbb{R}^{N \times D}$, it computes a weighted sum over all values \mathbf{v} in the sequence. The attention weights A_{ij} reflect the pairwise similarity between query \mathbf{q}_i and key \mathbf{v}_j representations of the input tokens.

$$\mathbf{q}, \mathbf{k}, \mathbf{v} = \mathbf{z} \mathbf{U}_{qkv} \quad \mathbf{U}_{qkv} \in \mathbb{R}^{D \times 3D} \quad (17)$$

$$\mathbf{A} = \text{softmax}\left(\frac{\mathbf{q}\mathbf{k}^T}{\sqrt{D}}\right) \quad \mathbf{A} \in \mathbb{R}^{N \times N} \quad (18)$$

$$\text{SA} = \mathbf{A}\mathbf{v} \quad (19)$$

Multihead self-attention (MSA) extends the self-attention mechanism by performing H parallel self-attention operations, where each self-attention is referred to as a “head”. The parameter H is a hyper-parameter that determines the number of heads. To ensure constant computation and parameter count with respect to H , the dimension D (Eq. 17) is set to $\frac{D}{H}$.

$$\text{MSA}(\mathbf{z}) = [\text{SA}_1(\mathbf{z}); \text{SA}_2(\mathbf{z}); \dots; \text{SA}_n(\mathbf{z})] \mathbf{U}_{msa} \quad \mathbf{U}_{msa} \in \mathbb{R}^{HD \times D} \quad (20)$$

A.3 Mask Analysis

In our ablation study, we examined the impact of masking and the choice between a fixed mask value or different mask values for each attention head. Three scenarios were considered: no mask, a fixed mask value for all heads, and different mask values for each head. Table 4 illustrates the advantages of employing distinct mask values for each head, highlighting the superiority over using a fixed mask value or no masking.

Models trained with masking generally demonstrate improved AUC compared to models without masking, as masking effectively eliminates irrelevant cross-features that can degrade prediction

Table 4: Ablation Study. Mask (θ) Analysis with Single Epoch Training - AUC Mean (std deviation). The ‘No Mask’ entry indicates a scenario containing no masking. The numbers in other entries show fixed mask values across all heads, and Ad-Rec employs different mask values across each head.

Model	Mask Value (θ)						
	No Mask	0.1	0.01	0.05	0.001	0.005	Ad-Rec
RM1	0.801095 (3.17e-4)	0.801269 (3.74e-4)	0.801357 (2.2e-4)	0.801055 (4.33e-4)	0.801112 (4.82e-4)	0.801199 (1.14e-4)	0.80153 (1.09e-4)
RM2	0.790164 (2.44e-4)	0.790222 (1.84e-4)	0.790214 (1.92e-4)	0.790176 (8.07e-5)	0.790185 (4.56e-4)	0.790179 (1.71e-4)	0.790224 (1.56e-4)
RM3	0.775091 (4.85e-4)	0.775081 (7.9e-4)	0.775044 (4.08e-4)	0.775344 (9.2e-4)	0.775637 (2.1e-4)	0.77587 (3.21e-4)	0.775971 (4.3e-4)
RM4	0.9453581 (2.88e-3)	0.9421871 (6.46e-3)	0.9465051 (2.57e-3)	0.9430625 (3.67e-3)	0.9434243 (4.54e-3)	0.9406334 (1.45e-3)	0.9494345 (1.9e-3)
RM5	0.8940437 (2.87e-4)	0.8938943 (2.93e-4)	0.89249 (2.04e-3)	0.8866167 (9.16e-3)	0.8882817 (5.43e-3)	0.8892716 (4.01e-3)	0.895358 (7.65e-3)
RM6	0.8500284 (1.73e-3)	0.840935 (8.25e-3)	0.8453409 (6.09e-3)	0.8424109 (6.67e-3)	0.8491047 (5.64e-3)	0.8374637 (4.19e-3)	0.8520705 (2.61e-3)
RM7	0.9323605 (1.45e-3)	0.9319719 (5.68e-3)	0.9326281 (1.05e-3)	0.9337075 (1.84e-3)	0.9317426 (8.62e-3)	0.9327804 (1.45e-3)	0.9404412 (1.82e-3)

quality. However, determining the optimal mask threshold presents a challenge. Different models require different mask thresholds (θ), and selecting an unsuitable mask can harm prediction quality by eliminating important features. Prior approaches [Liu et al., 2020, Khawar et al., 2020, Zhu et al., 2021] tackle this issue by training models specifically to learn such features, but this approach incurs computational costs and lacks generalizability across models or even the same model with different sizes. In contrast, Ad-Rec addresses this challenge by utilizing different mask values for each attention head, facilitating better generalization. If an important feature is eliminated in one head, it can be compensated for by other attention heads, resulting in a higher-quality model.

A.4 Positional Embedding

In our sensitivity study, we explored different ways of encoding the spatial information of features using positional embeddings inspired by NLP models. We considered two cases:

- **No positional information:** This case involved using only feature embeddings and providing them as-is to the transformer encoder. This approach was the default across all other experiments in the paper.
- **1-dimensional positional embedding:** We treated the input features as a sequence of features, assigning each sparse feature and dense feature vector a position based on the embedding table position for language models. We added position embeddings to the feature inputs just before feeding them to the Transformer encoder. The dimension of the position embedding was kept similar to the sparse feature dimension, and the number of position embeddings was equal to the number of features.

Equation 21 demonstrates the incorporation of positional embeddings into the input features. The feature inputs and their respective embeddings were summed with the position embeddings.

$$\mathbf{z}_0 = [\text{MLP}(\mathbf{x}_{\text{dense}}); \mathbf{x}_{\text{sparse}}^1 \mathbf{E}^1; \dots; \mathbf{x}_{\text{sparse}}^N \mathbf{E}^N] + \mathbf{E}_{\text{pos}} \quad \mathbf{E} \in \mathbb{R}^{M \times D}, \mathbf{E}_{\text{pos}} \in \mathbb{R}^{(N+1) \times D} \quad (21)$$

Table 5 presents the evaluation results comparing the models with and without positional embeddings. Our hypothesis was that since the Multi-Head Attention block exhibits permutation-equivariance, the position of a feature in the input sequence does not encode useful information. Therefore, the models that directly input the raw features to the masked transformer encoder, facilitating higher-order feature interaction, performed the best. Incorporating 1-dimensional positional embeddings led to a degradation in model performance, even worse than the DLRM baseline. Notably, in certain models like RM3, incorporating 1-dimensional positional embeddings prevented the model from converging.

Table 5: Results of ablation study on positional embeddings with single epoch training.

Model	AUC		Test Accuracy (%)		BCE Loss	
	No Pos. Emb.	1-D Pos. Emb.	No Pos. Emb.	1-D Pos. Emb.	No Pos. Emb.	1-D Pos. Emb.
RM1	0.801	0.796	78.70	78.34	0.455	0.461
RM2	0.790	0.786	81.22	80.94	0.423	0.426
RM3	0.775	Not Converge	83.76	Not Converge	0.382	Not Converge

Figure 8 illustrates that recommendation models achieve convergence in significantly fewer training iterations when no spatial information is added to the input feature embeddings. Even the model with 1-dimensional positional embedding requires more training iterations than the baseline DLRM with second-order cross-features to reach the target AUC.

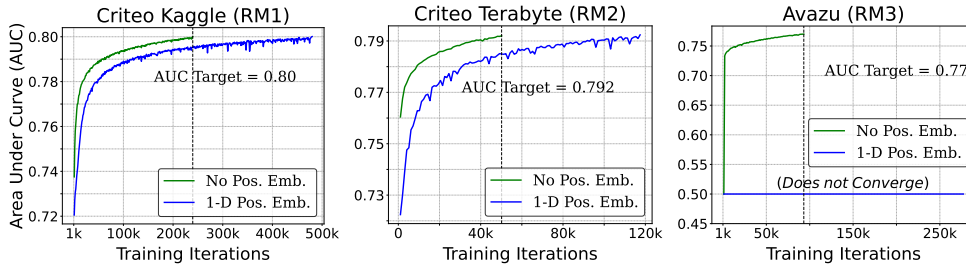


Figure 8: Model convergence with and without positional embedding.

A.5 Ad-Rec: Masked Transformer Hyper-parameters Analysis

To evaluate the robustness of our Ad-Rec model, we conducted an extensive study by varying the hyperparameters of the transformer encoder. Table 6 provides an overview of the different hyperparameters considered in this sensitivity analysis.

Table 6: Scaling hyper-parameters of transformer encoder.

Num Layers	Num Heads	Dropout Ratio	Non-Linear Activation	Hidden Size	Linear Config.
N	H	D	A	d_{model}	d_{ff}
1	1	0.01	ReLU	16	128
2	2	0.05	GeLU	64	512
4	4	0.1			
	8	0.2			
	16	0.3			

A.5.1 Number of Layers

We investigated the impact of the number of masked transformer layers (N) in the RM1 model while keeping other hyperparameters constant. Figure 9 showcases the test accuracy and BCE loss for the RM1 model. Our observations revealed that increasing the number of masked transformer layers did not yield significant benefits due to the smaller sequence length of RM1 (27 features). However, we anticipate that models with a larger number of features and longer sequence lengths would demonstrate improved AUC with more masked transformer layers. This is because higher-order feature interaction becomes more valuable when there are more features. In large-scale industrial datasets, the number of sparse features can reach thousands. For instance, the Meta synthetic dataset¹, which cannot be used for training due to its synthetic nature, contains 856 sparse features. Nevertheless, it highlights the scale at which Ad-Rec can significantly enhance prediction accuracy.

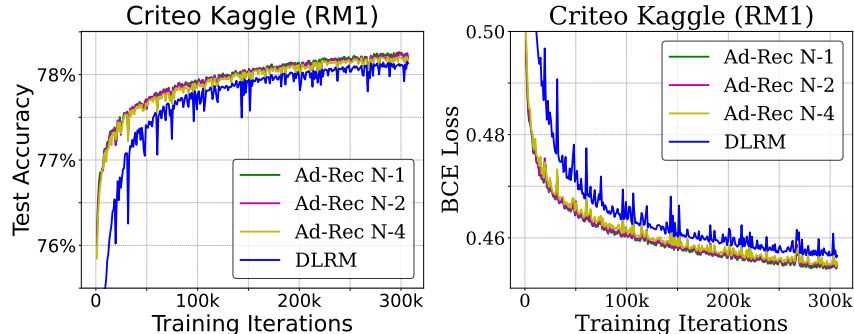


Figure 9: Test Accuracy and BCE Loss with varying layers of Ad-Rec masked transformer.

¹https://github.com/facebookresearch/dlrm_datasets

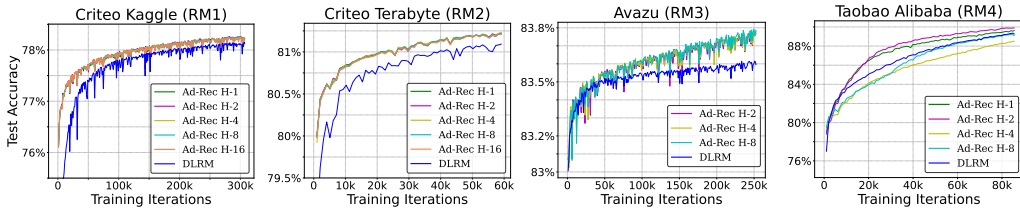


Figure 10: Trends in test accuracy by varying the number of attention heads of masked transformer for RM1, RM2, RM3, and RM4 models. Models with missing head (RM3 and RM4 with 16 heads) means the model could not converge.

A.5.2 Number of Attention Heads

We employ masked multi-head attention to enable higher-order feature interactions across multiple subspaces. This technique divides a single embedding vector into multiple heads of the same length, allowing for parallel execution and feature interaction within different subspaces. The number of attention heads (H) varies from 1 to 16 for each model (RM1, RM2, RM3, and RM4). The relationship between the test accuracy and the number of attention heads is illustrated in Figure 10. Notably, the computational complexity remains unchanged as all the heads are concatenated at the end, and each head operates on a portion of the embedding vector.

Our observations indicate that models with an intermediate number of heads consistently converge and yield higher accuracy. In contrast, the RM3 model fails to converge when using a single-head model, emphasizing the importance of feature interaction in multiple subspaces. Furthermore, when the number of heads equals the length of the embedding vector D (i.e., $H = D$), the feature interaction becomes excessively fine-grained, leading to model divergence. For the RM3 and RM4 models, it was observed that neither model converged when using ($H = 16$) and ($D = 16$), reinforcing the need for an appropriate balance in the number of attention heads to achieve optimal performance.

A.5.3 Dropout Ratio

The masked transformer architecture incorporates a residual connection, depicted in Figure 2a, to ensure effective information flow and gradient propagation. Additionally, a dropout mechanism prevents overfitting by randomly replacing input features with random features. To investigate the impact of the dropout ratio on model predictions, we varied the ratio across all models, ranging from 0.01 to 0.3.

Figure 11 showcases the relationship between the dropout ratio and test accuracy. Our findings consistently demonstrate that lower dropout values (0.01 - 0.05) yield superior predictions across all models. These smaller dropout ratios enable cross-features to incorporate with the original raw features, facilitating improved learning of implicit interactions. As the dropout ratio increases, the test accuracy gradually declines, eventually approaching the performance of the baseline DLRM model when the dropout ratio reaches 0.3.

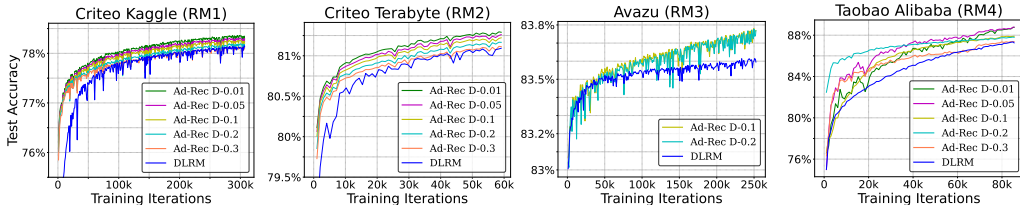


Figure 11: Trends in test accuracy by varying dropout ratio of residual connection in masked transformer for RM1, RM2, RM3, and RM4 model. Models with missing dropout values (RM3 with a dropout of 0.01 and 0.05) mean the model could not converge.

The diminishing test accuracy with higher dropout ratios can be attributed to introducing more random features into the cross-features. These additional random features may disrupt the underlying patterns and relationships in the data, negatively impacting model performance. This finding aligns with previous research [Song et al., 2019], which utilizes raw features without dropout in multi-head attention-based cross-features to learn higher-order interactions. However, in the case of Ad-Rec, a smaller dropout ratio is employed during training to enhance generalization, while dropout is removed during inference for optimal performance.

A.5.4 Non-Linear Activation

Figure 12 presents the investigation into the impact of non-linear activation functions on test accuracy. Surprisingly, transitioning from the default ReLU activation to GeLU activation does not yield any noticeable effect on the test accuracy of the models. Regardless of the chosen non-linear activation function, all models across different datasets converge to the same point.

This finding suggests that the specific type of non-linearity employed in the activation function does not significantly influence the extraction of cross-features. It indicates that the masked transformer architecture is robust to different non-linearities, and the models can effectively capture and learn the underlying interactions between features regardless of the specific activation function used.

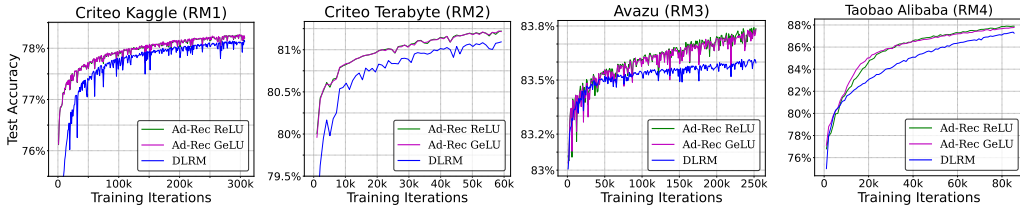


Figure 12: Trends in test accuracy by changing the non-linear activation of a feed-forward network of the masked transformer. It does not have any effect on the model quality.

A.6 Attention Heads Masking Analysis

We randomly sampled test samples from each dataset to examine the impact of masking on each attention head and its role in enhancing predictions by eliminating irrelevant features. We then plotted the attention weights for each attention head with and without a mask. Figures 14, 15, and 16 showcase the attention weights for the RM1, RM2, and RM3 models, respectively. These plots provide insights into how different attention heads learn feature interactions in multiple subspaces and how attention weights vary across different attention heads. By employing different mask values for each attention head, masking selectively masks out attention weights of irrelevant features, redistributing the attention weight across other relevant features accordingly.

Sequential Embedding Vectors’ Feature Interaction: The quality of sequence embedding vectors (Z) plays a crucial role in the prediction quality of sequential recommendation. To better understand the patterns within these vectors, we utilize Principal Component Analysis (PCA) to map the embedding vectors (with a width of 16) into a 2-dimensional space. In this space, similar interactions are grouped closely together, while dissimilar interactions are distanced apart. The proximity of the next item’s placement to historical item interactions indicates a higher probability of the user clicking on that item. Figure 13 depicts the PCA plot for sequential embedding vectors generated by both feature interaction methods, as explained in Section 4. Each method generates 21 embedding vectors, representing the user’s historical interactions, with the next item represented by a star symbol (\star).

In the plot, closely related interactions form clusters, and the relative Euclidean distance between clusters signifies their correlation. For DLRM-based feature interaction, we observe that all sequential interactions are clustered together, resulting in four closely located clusters in the Euclidean space. On the other hand, Ad-Rec-based feature interaction generates more distinct clusters based on the type of user interactions. The sequential layer predicts the likelihood of the user clicking on the next item vector based on the placement of the next item embedding in relation to the user’s sequential embedding vectors.

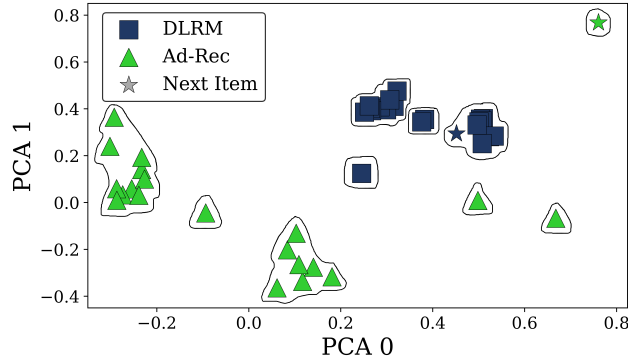


Figure 13: Principal Component Analysis (PCA) to represent high-dimensional sequential user activity in 2-dimensional space. This compares DLRM and Ad-Rec generated embedding vectors for the RM4 model. Note that the next item (denoted by \star) is a *negative sample*. Thus, a *large Euclidean distances* between the next item and sequential interaction clusters indicate a higher quality model.

Criteo Kaggle (RM1)

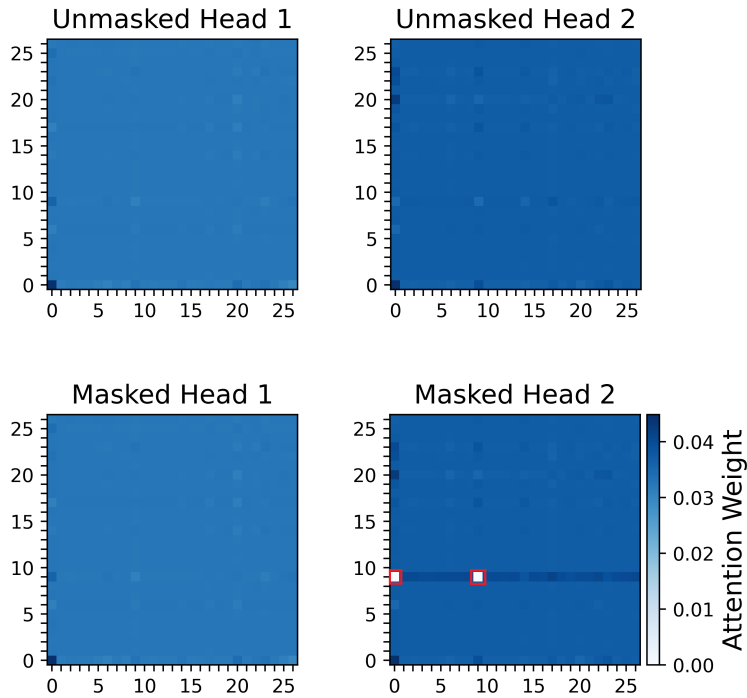


Figure 14: Attention Weights for **RM1** model across 2 heads. The unmasked head contains original attention weights, while the masked head contains attention weights after masking. X and Y axes contain 27 features with 0 as dense feature vectors while others are sparse feature vectors. Highlighted features are the masked features that are irrelevant.

Interestingly, we notice that Ad-Rec-based feature interaction generates an embedding vector for the next item that is situated far away from previous user interactions, indicating that the next item does not have a strong connection to the user’s sequential interactions. Conversely, for DLRM-based feature interaction, the next item is located within the cluster, suggesting a close relationship with most previous interactions. The placement of Ad-Rec-generated sequence vectors and subsequent item vectors aligns with the ground truth, as the input represents a negative sample.

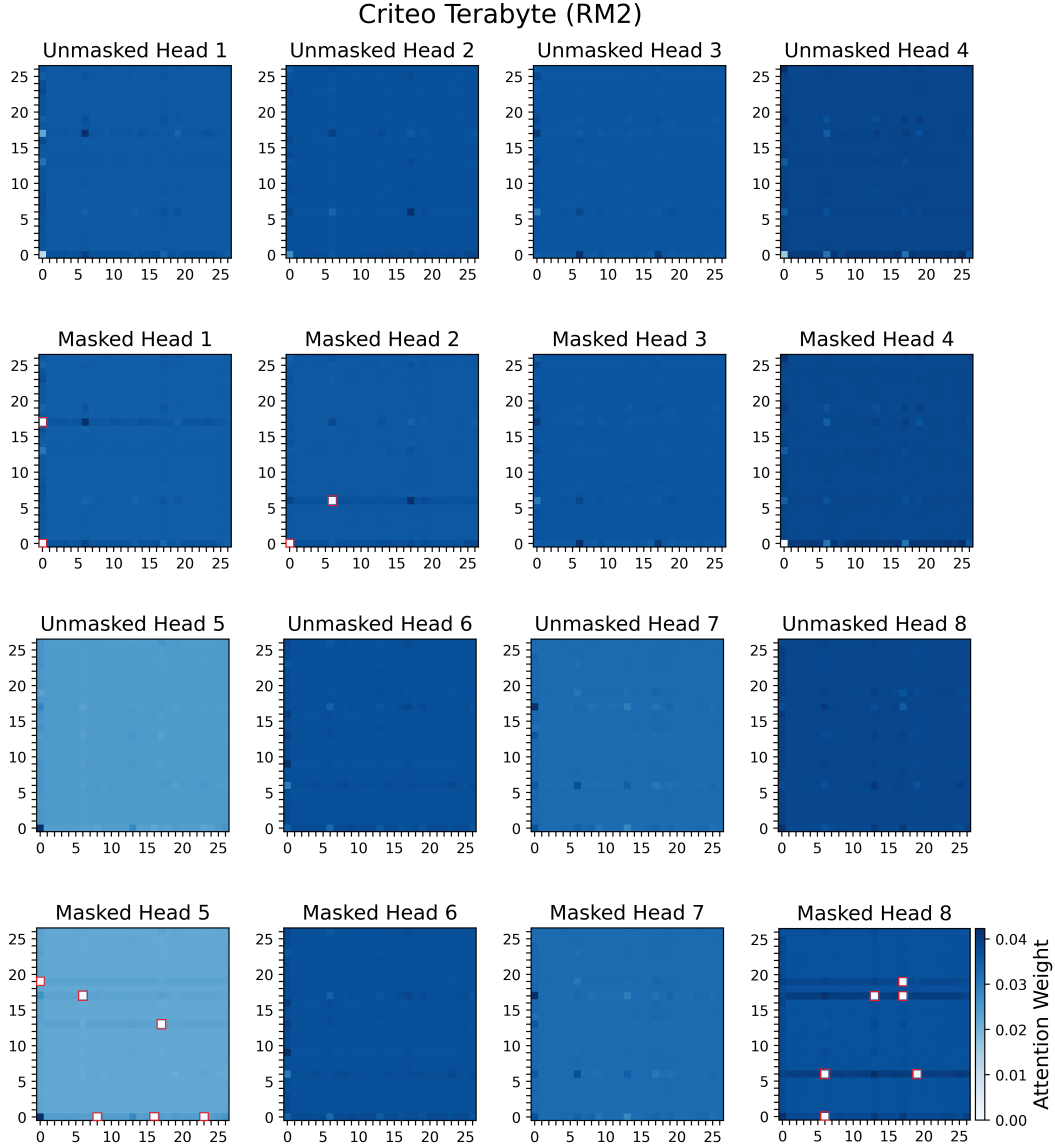


Figure 15: Attention Weights for **RM2** model across 8 heads. The unmasked head contains original attention weights, while the masked head contains attention weights after masking. X and Y axes contain 27 features with 0 as dense feature vectors, while others are sparse feature vectors. Highlighted features are the masked features that are irrelevant.

A.7 Scaling laws of Recommendation Models

To investigate the scaling laws of recommendation models, we conducted experiments by scaling various model components. Table 7 provides an overview of the scaled components and their corresponding configurations, along with the model size in terms of parameters. This analysis allows us to assess the impact of scaling on model quality.

Previous research [Ardalani et al., 2022] has explored the scaling laws for non-sequential recommendation models, particularly focusing on Click-Through Rate (CTR) in DLRM-style models. Their findings revealed that increasing the model size did not significantly enhance accuracy, while training on more data led to slight improvements.

In contrast, Figure 7 demonstrates the behaviour of model loss as different components, including the Ad-Rec loss, are scaled. Interestingly, even with fewer parameters (approximately half), Ad-Rec

Avazu (RM3)

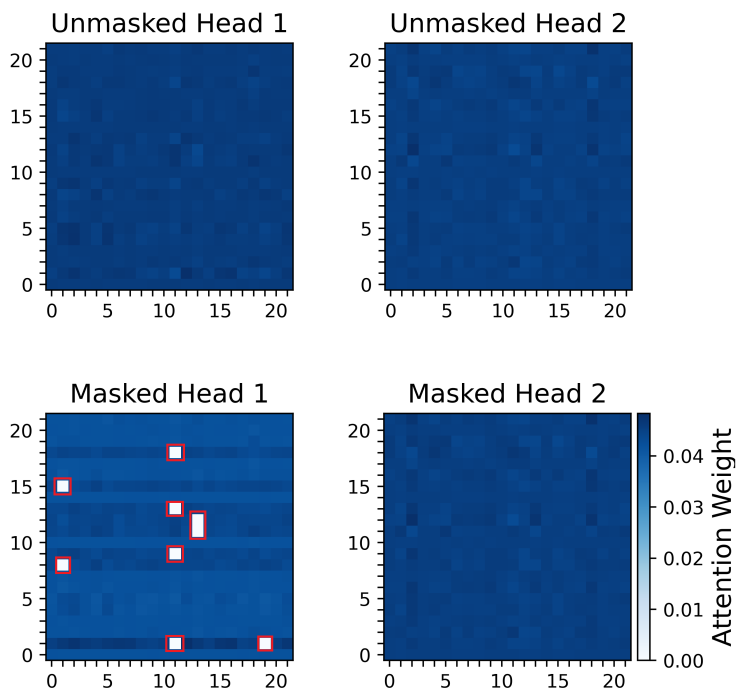


Figure 16: Attention Weights for **RM3** model across 2 heads. The unmasked head contains original attention weights, while the masked head contains attention weights after masking. X and Y axes contain 22 features with 0 as dense feature vectors, while others are sparse feature vectors. Highlighted features are the masked features that are irrelevant.

outperforms other models regarding convergence speed. This emphasizes the significance of higher-order feature interaction, eliminating irrelevant features, and addressing covariate shifts in improving the representation of input features. Merely scaling existing components or increasing the size of training datasets does not yield comparable results. The success of Ad-Rec opens up new avenues for research in recommendation model architecture.

Table 7: Scaling Recommendation Models Components

Model	Scaling Component	Sparse Dimension	Neural Network Configuration		Model Parameters
			Bottom MLP	Top MLP	
RM1	(N/A) DLRM	16	13-512-256-64-16	512-256-1	540.7M
RM1	(N/A) Ad-Rec	16	13-512-256-64-16	512-256-1	540.8M
RM1	Sparse Emb. Dim	32	13-512-256-64-32	512-256-1	1.08B
RM1	Top MLP	16	13-512-256-64-16	1024-768-512-256-1	542.1M
RM1	Bottom MLP	16	13-1024-768-512-256-128-64-16	512-256-1	542M
RM1	All Comp.	32	13-1024-768-512-256-128-64-32	1024-768-512-256-1	1.08B
RM2	(N/A) DLRM	64	13-512-256-64	512-512-256-1	2.7B
RM2	(N/A) Ad-Rec	64	13-512-256-64	512-512-256-1	2.701B
RM2	Sparse Emb. Dim	128	13-512-256-128	512-512-256-1	5.399B
RM2	Top MLP	64	13-512-256-64	1024-768-512-512-256-128-1	2.701B
RM2	Bottom MLP	64	13-1024-768-512-256-128-64	512-512-256-1	2.701B
RM2	All Comp.	128	13-1024-768-512-256-128	1024-768-512-512-256-128-1	5.401B
RM3	(N/A) DLRM	16	1-512-256-64-16	512-256-1	150.24M
RM3	(N/A) Ad-Rec	16	1-512-256-64-16	512-256-1	150.37M
RM3	Sparse Emb. Dim	32	1-512-256-64-32	512-256-1	300.08M
RM3	Top MLP	16	1-512-256-64-16	1024-768-512-256-128-64-1	151.59M
RM3	Bottom MLP	16	1-1024-768-512-256-128-64-16	512-256-1	151.44M
RM3	All Comp.	32	1-1024-768-512-256-128-64-32	1024-768-512-256-128-64-1	302.64M
RM4	(N/A) DLRM	16	1-16	15-15	82.55M
RM4	(N/A) Ad-Rec	16	1-16	15-15	82.57M
RM4	Sparse Emb. Dim	32	1-32	15-15	165.10M
RM4	Top MLP	16	1-16	32-15-15	82.55M
RM4	Bottom MLP	16	1-8-16	15-15	82.55M
RM4	All Comp.	32	1-16-32	32-15-15	165.10M